Analysis of fatigue crack growth in a rubber-toughened epoxy resin: effect of temperature and stress ratio

Moustafa Abou-Hamda, Yiu-Wing Mai* and Shang-Xian Wu
Centre for Advanced Materials Technology, Department of Mechanical Engineering, University of Sydney, New South Wales 2006, Australia

and Brian Cotterell
School of Mechanical and Production Engineering, National University of Singapore, Singapore
(Received 27 August 1992; revised 25 January 1993)

Fatigue crack propagation in a rubber-toughened epoxy resin was studied at different test temperatures (−40 to 60°C) and stress ratios (0.05 to 0.70) using single edge-notched specimens at a frequency of 5 Hz. Fatigue crack propagation rates (da/dN) were plotted against the stress-intensity factor amplitude (ΔK) in accordance with the Paris power-law equation. For a given stress ratio da/dN was not sensitive to variations in test temperature. But for a given temperature da/dN increased with stress ratio. Using the Williams' two-stage line zone model to analyse these experimental data, it was shown that the main failure process was due to shear plastic flow at the crack tip. The fatigue stress and the closure stress-intensity factor both decreased with increasing temperature, implying that more severe damage had occurred at higher testing temperatures. The experimental data were also analysed in terms of a new fatigue model, which considers the accumulation of damage due to cyclic plastic strain in the reversed plastic zone similar to the Coffin–Manson law and crack closure due to residual plastic stretch at the crack wake. There was good agreement between theory and experiment, suggesting a simpler way to correlate fatigue crack growth rates in this and other polymeric materials.

(Keywords: fatigue crack propagation; rubber-modified epoxy; stress ratio; damage accumulation; crack closure; Coffin–Manson law; fatigue models)

INTRODUCTION

The motivation of using rubber-toughened epoxy, in high-strength, high-performance structural components, both as an adhesive and as a matrix binder for modern composites, has been increasing in recent years. The all-round performance is attributed to the two-phase nature of the system, which makes possible toughening mechanisms that do not occur in a single-phase material[1–3]. Failsafe design philosophy requires that such resins must withstand cyclic or repeated loading, which is inherently more damaging than corresponding monotonic loading. Some of the factors affecting fatigue properties are stress ratio, temperature, frequency, loading characteristic waveform, environmental effects, humidity and method of testing[4]. Most previous studies have involved monotonic loading properties, such as impact strength or fracture toughness, which emphasize the toughening mechanisms that greatly increase the resistance to crack growth[5–10]. However, relatively little work has been conducted on the fatigue crack growth behaviour in both neat and rubber-modified epoxies[11–17]. A review of these published works shows that they are mainly concerned with the role of the rubbery phase, its composition and optimum content in improving the fatigue resistance, as well as the characterization of the fatigue crack growth behaviour from crack initiation to stable propagation and to final instability.

Results obtained on the neat resin diglycidyl ether of bisphenol A (DGEBA) 4,4′-methylenedianiline (Epon 828 MDA) showed that the fatigue crack growth (FCG) rate, da/dN, closely followed the Paris power-law equation[12], i.e. $da/dN \propto \Delta K^m$, where ΔK is the stress-intensity factor range and m is an exponent depending on the testing conditions. Sutton[11] found a better correlation between da/dN and the elastic-energy release rate range ΔG rather than the stress-intensity factor range ΔK. He showed that empirically in this way a single equation could be used to describe all the da/dN data independently of the mean stress-intensity factor. No fatigue marking was observed on the fracture surface. In contrast Kim *et al.*[12] showed that fatigue crack growth could be correlated with fracture surface morphology and stable cyclic crack growth was represented by shiny areas where fatigue striation could be observed[12]. However, for unstable tensile fractures, tearing marks and parabolic imprints were found in both studies[11,12].

*To whom correspondence should be addressed

0032-3861/93/204221-09

To investigate the effect of rubber inclusions, Shah *et al.*[14] carried out both monotonic and cyclic loading tests on a carboxyl-terminated butadiene–acrylonitrile rubber (CTBN) modified DGBA (DER 311, Dow Chemical Co.) epoxide resin. Their results showed yielding and toughening under monotonic loading but no toughening was observed under tensile fatigue loading. Such a paradoxical observation was explained in terms of the two competing mechanisms: matrix plasticity, which decreased *FCG* rate, and reduced elastic modulus, which increased *FCG* rate. However, more recent work by Hwang *et al.*[16] found that rubber did improve the *FCG* resistance after carrying out their tests on epoxies containing epoxy-terminated butadiene–acrylonitrile rubber (ETBN) and amino-terminated butadiene–acrylonitrile rubber (ATBN) (though CTBN was not studied). They also concluded that the fatigue life of these epoxies could be extended from two to seven times by the addition of rubber. Stress whitening was observed visually in the stable crack growth region for the series of low glass-transition-temperature T_g epoxies, which showed both interfacial debonding and cavitation within the rubber particles. An increase in the *FCG* rate with increasing frequency was noted and rationalized by strain-rate effects as suggested by Kinloch[7] and Yee[8]. In addition they found that the *FCG* resistance increased with increasing temperature and apparent molecular weight between the crosslinks of the matrix. The explanation of the former effect is that the fracture toughness K_{Ic} and G_{Ic} increase with temperature until about the glass transition temperature T_g. The latter results are a consequence of the relaxation of the polymer chains and viscoelastic motion during such loading[18].

Finally, theoretical modelling of the *FCG* behaviour of rubber-modified epoxies is found wanting. Most previous studies, like the neat resins, express the fatigue crack growth rate using the same empirical formula developed by Paris[19]. Attempts[16] to include other variables such as frequency, temperature, yield strength and modulus did not make any significant advances. Recently, Wang *et al.*[17] have applied the crack layer theory to evaluate the crack-tip damage and its evolution during stable cyclic crack growth, from initiation to ultimate failure with the aid of fractal analysis of the fracture surfaces.

Since cyclic crack growth occurs at stresses below those required for static fracture, it is necessary to understand the accumulation of damage leading to eventual failure. Therefore, the use of empirical formulae such as the Paris equation will not give any physical insight into the fracture process during cyclic loading. Consequently, there are very few *FCG* models that can be directly applied to calculate the *FCG* data owing to different testing variables.

In the present paper, a realistic model, in terms of a critical crack-opening displacement and a Dugdale two-stage line zone in which fatigue damage accumulates, originally developed by Williams[20], and further expanded by Mai and Williams[21], Osorio and Williams[22] and Yap *et al.*[23] to include the effects of stress ratio, crack closure and liquid environment, is applied to analyse the fatigue crack growth data for a CTBN-modified epoxy resin tested at a range of stress ratios and temperatures. Moreover, the application of a new mechanistic model proposed by Wu *et al.*[24] based on the modified Dugdale model considering crack closure and damage accumulation due to the cyclic plastic strain in the crack tip reversed plastic zone was also presented. The relative merits of these two models are discussed.

EXPERIMENTAL

The compositions of the rubber-toughened epoxy resin were: an epoxy GY 250 (Ciba-Geigy Araldite), which is diglycidyl ether of bisphenol A (DGEBA) with a molecular weight of 300 (100 parts); a liquid rubber Hycar CTBN 1300×13 (B.F. Goodrich Co.), which has an acrylonitrile content of 27%, a carboxyl content of 2.4% and a mean molecular weight of 3400 (15 parts); and a secondary amine hardener, piperidine (5 parts). All the samples were made following the procedures described in earlier work by Mai and coworkers[9,10] and this allowed specimens with dimensions $70 \times 200 \times 6\,mm^3$ to be machined from the moulded sheets. All the samples were the single edge-notched (SEN) geometry. The glass transition temperature for the resultant material was determined using differential scanning calorimetry and was found to be about 70°C. The average rubber particle size was 1.0 μm as revealed by the osmium staining technique.

Fatigue crack growth experiments were conducted in a Shimadzu Servo-Pulser at 5 Hz with varying stress ratios and a range of temperatures from −40 to 60°C using an Instron temperature cabinet with thermostat control to ±1°C accuracy. Crack length measurements were based on the computer-aided automated system developed by Mai and Kerr[25,26] using electrically conductive surface grids obtained by the screen printing technique. All the bars were about 0.12 mm wide and 1 mm apart from each other. The accuracy of the test method was compared with the optical technique using a travelling microscope for each test temperature. Correction factors to the actual crack length due to the curvature of the crack front were added to the computer-recorded length when necessary. Simple programs were written to generate da/dN (fatigue crack growth rate) *versus* ΔK (stress intensity factor range) curves from these raw data. The stress-intensity factor amplitude (ΔK) is given by:

$$\Delta K = \Delta\sigma\sqrt{a}Y \quad (1)$$

where $\Delta\sigma$ is the stress amplitude, a is the crack length and Y is the correction factor for the SEN geometry and a function of relative crack length (a/W). W is the specimen width here.

RESULTS AND DISCUSSION

Effect of temperature and stress ratio

The effects of stress ratios on fatigue crack growth rates at test temperatures between 60 and −40°C have been studied, and typical results at a stress ratio $R = 0.1$ are shown in *Figure 1*. It is difficult to identify a definite trend of the temperature effect. However, other studies[16] on rubber-toughened epoxy conducted at 1 and 20 Hz show that raising the temperature appears to increase the *FCG* resistance, as described for most rubber-toughened polymers including epoxies[27,28]. The possible factors causing such a difference between the literature and the current results might be caused by the

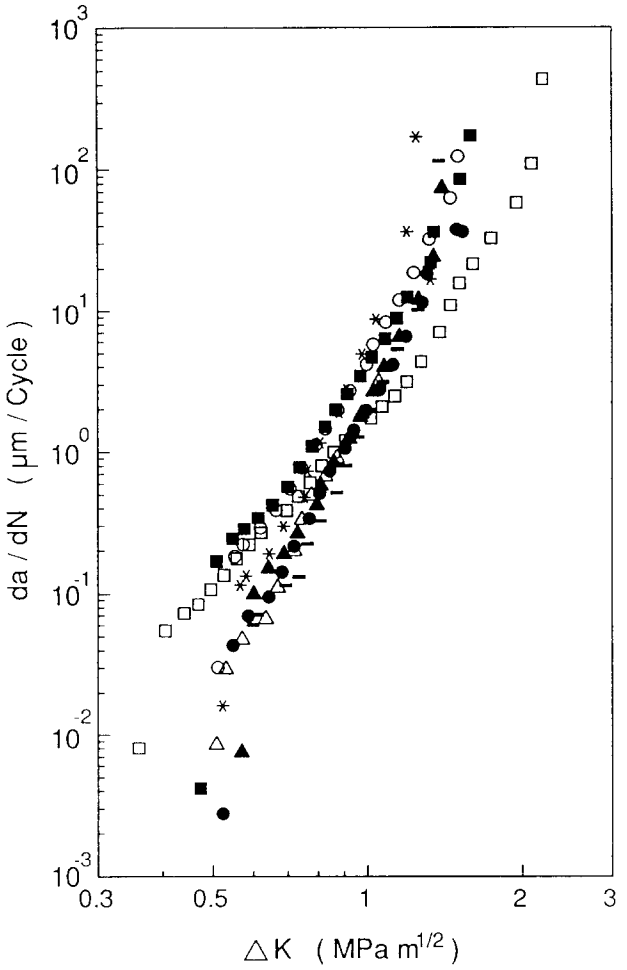

Figure 1 The effect of temperature on fatigue crack growth at $R=0.1$ in a rubber-toughened epoxy resin: $T=60°C$ (□), 50°C (■), 40°C (○), 30°C (●), 20°C (△), 0°C (▲), −20°C (*), −40°C (-)

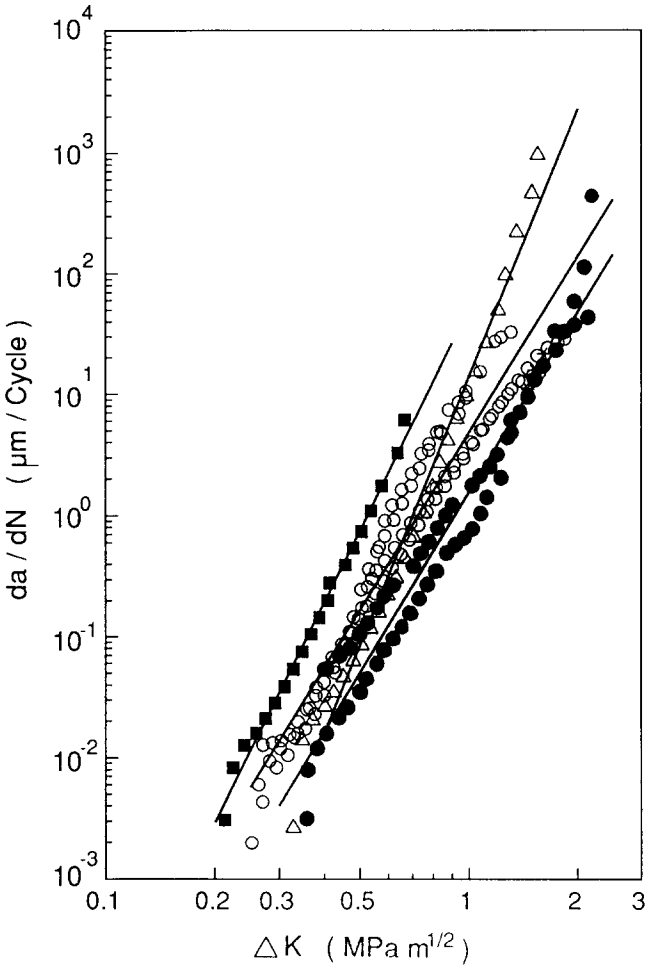

Figure 2 The effect of stress ratio on fatigue crack growth at $T=60°C$ in a rubber-toughened epoxy resin: $R=0.1$ (●), 0.2 (△), 0.5 (○), 0.7 (■)

differences in the resin molecular weight, cyclic frequency and experimental control including loading waveform. However, as typified by the experimental data in *Figure 2*, at each test temperature the fatigue crack growth rate is dependent on the stress ratio. Generally, the higher the stress ratio, the higher is the fatigue crack growth rate, and this trend is more clearly shown at the higher temperatures of 60 and 40°C. These experimental data are best fitted to the Paris power-law equation:

$$da/dN = A(\Delta K)^m \quad (2)$$

where A and m are given in *Table 1* for different test temperatures and stress ratios.

However, it is observed in *Figures 1* and *2* that there exists a minimum intensity factor amplitude, ΔK_{th}, below which fatigue crack growth is negligible. It also appears that ΔK_{th} decreases with increasing stress ratio and temperatures. Clearly, equation (2) cannot be used to describe the near-threshold fatigue crack growth data.

The advantage of incorporating rubber into pure epoxy resin on the fatigue crack growth is clearly indicated in *Figure 3* at ambient temperature (30°C) and stress ratio 0.1. Results obtained by Sutton[11] and Manson *et al.*[15] for a pure and rubber-roughened epoxy resin are also superimposed in this figure.

In principle, da/dN approaches infinity as the maximum stress-intensity factor, K_m, approaches the fracture toughness, K_{1c}, of the material. Thus using the

Table 1 Constants A and m of the Paris power-law equation for fatigue crack growth in a CTBN-modified epoxy resin (da/dN in μm/cycle and ΔK in MPa $m^{1/2}$)

Temperature (°C)	Stress ratio, R	A	m
60	0.05	3.93	6.12
	0.10	1.55	4.95
	0.20	13.82	7.32
	0.50	12.83	5.94
	0.60	564.87	5.97
	0.70	48.61	6.04
50	0.10	9.22	5.60
40	0.05	5.38	5.43
	0.10	5.35	6.27
	0.30	14.06	6.27
	0.50	75.25	7.16
	0.60	133.27	6.38
	0.70	3768.00	8.95
30	0.10	3.59	6.45
20	0.05	1.15	5.67
	0.10	2.29	7.09
	0.50	20.73	6.82
0	0.10	2.37	6.39
−20	0.05	3.15	6.47
	0.10	6.14	7.62
	0.50	64.13	7.90
−40	0.10	1.66	6.67

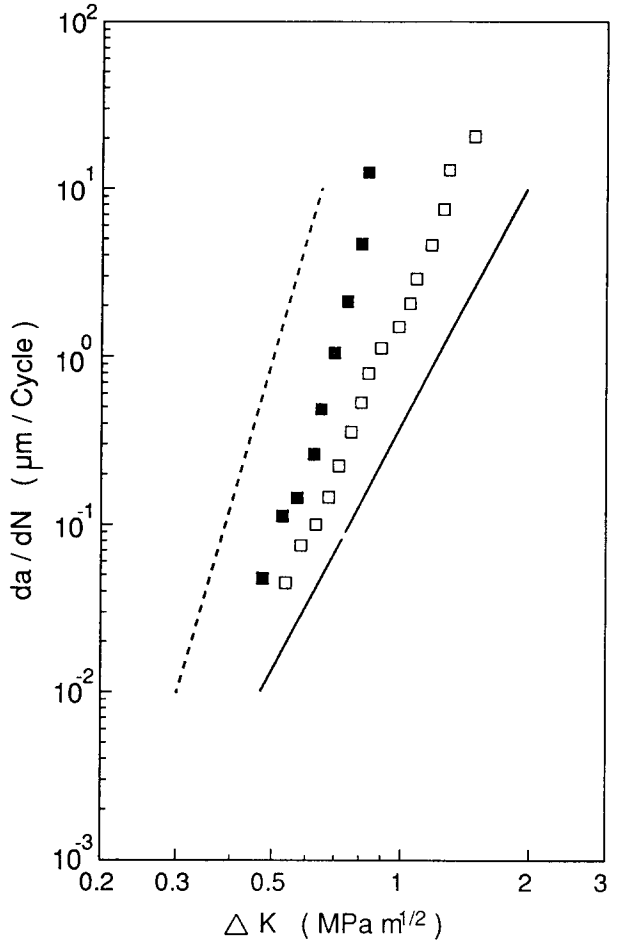

Figure 3 Comparison with results of other researchers: pure epoxy[15] (■); rubber-toughened epoxy[15] (□); rubber-modified epoxy[15] (——); epoxy[11] (– – –)

last data point of the *FCG* curves as K_m, after which the crack becomes unstable, *Figure 4* compares these values obtained in cyclic fatigue with the static fracture toughness (K_{Ic}) measured in monotonic loading[9,10]. Quite clearly, K_m is considerably less than K_{Ic}, particularly at temperatures above −20°C. This observation is probably associated with the fact that in cyclic fatigue the effective strain rate is much lower than in the monotonic fracture toughness test. In addition, the amount of damage accumulated at the fatigue crack tip is much larger than at a razor-notched crack tip for fracture toughness measurements.

Theoretical analysis of FCG *data*

Williams' two-stage line zone model. As proposed by Williams and coworkers[20–23], the fatigue crack growth rate is given by:

$$\frac{da}{dN}=\frac{\tau}{8(1-\alpha)^2\sigma_0^2}[F(R)(K^2-K_0^2)-\alpha(\delta_c\sigma_0 E)] \quad (3)$$

where $\alpha=\sigma_c/\sigma_0$ is related to the damage factor f by $\alpha=(1-f)+fR^2$, σ_0 is the yielding (or crazing) stress, σ_c is the damage stress due to cyclic fatigue, K_0 is the crack closure stress-intensity factor, and δ_c is the critical opening displacement. $F(R)$ is dependent on the damage processes occurring at the crack tip during cyclic fatigue and is a function of the stress ratio R. Despite the criticism of the assumption of a constant crack-tip opening displacement criterion during cyclic fatigue fracture[29], the model does give a sound physical basis for the description of the fatigue process in polymers. The following are analyses of the fatigue crack growth data at 60 and 40°C at different stress ratios. *Figure 5* shows all the data at 40°C and 5 Hz plotted in accordance with equation (3). However, the material parameters such as δ_c, σ_0, ΔK_{th} and α can only be obtained by analysis of the fatigue data in the low-growth-rate region to exclude the effect of viscoelastic crack growth. *Figure 6* shows the data in the region below 0.5 μm/cycle. (Using data up to 1–2 μm/cycle does not lead to any large variations in the material parameters.) From these results we can obtain the slope (S) and intercept (I) of the curves at different ratios R. Thus:

$$S=\frac{\pi}{8(1-\alpha)^2\sigma_0^2}F(R) \quad (4)$$

$$I=\frac{\alpha(\delta_c\sigma_0 E)}{F(R)}+K_0^2=K_{th}^2 \quad (5)$$

$$SI=\frac{\pi}{8}\frac{E\delta_c}{\sigma_0}\frac{\alpha}{(1-\alpha)^2}+K_0^2 S \quad (6)$$

Figure 7 is a plot of SI against S and using the slope of the least-squares straight line the closure stress-intensity factor $K_0=0.30$ MPa m$^{1/2}$. Admittedly, the correlation of the data in *Figure 7* is not good. But even if the data point (0.138, 1.0) is excluded and the correlation becomes much better (i.e. broken line in the figure), K_0 is only about 10% higher. However, we feel that this

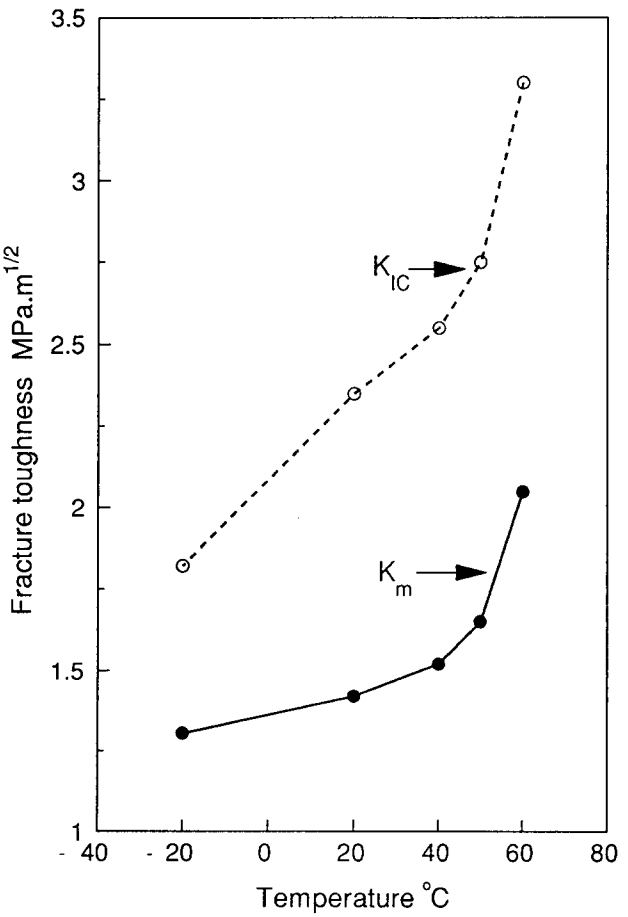

Figure 4 Variation of fracture toughness with temperature: fatigue tests (—●—); fracture tests (– –○– –)

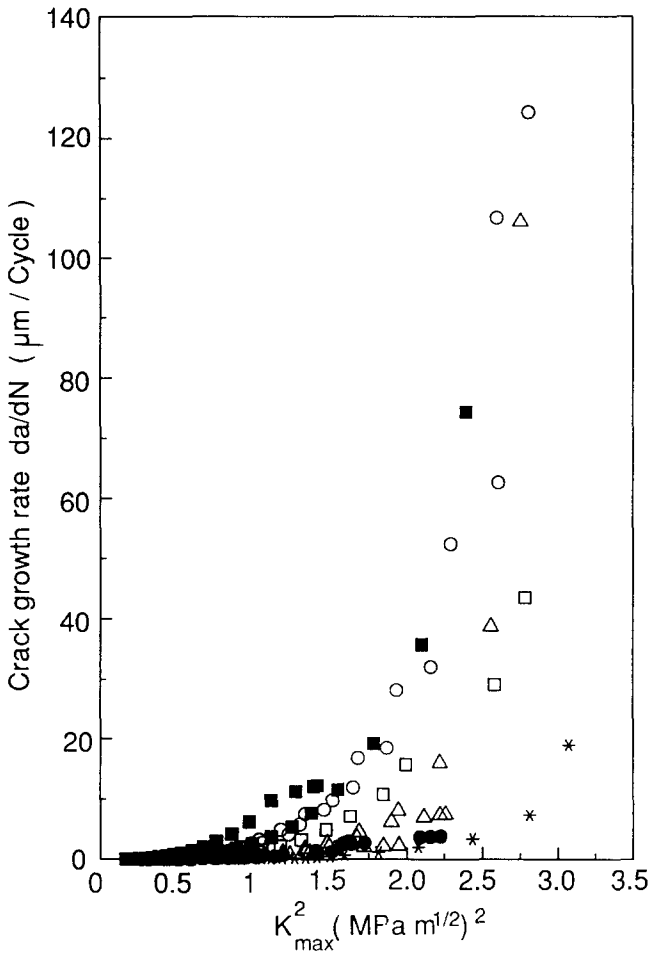

Figure 5 Fatigue crack growth data for rubber-toughened epoxy resin at 40°C and 5 Hz: $R=0.05$ (■), 0.1 (○), 0.3 (□), 0.6 (△), 0.7 (*)

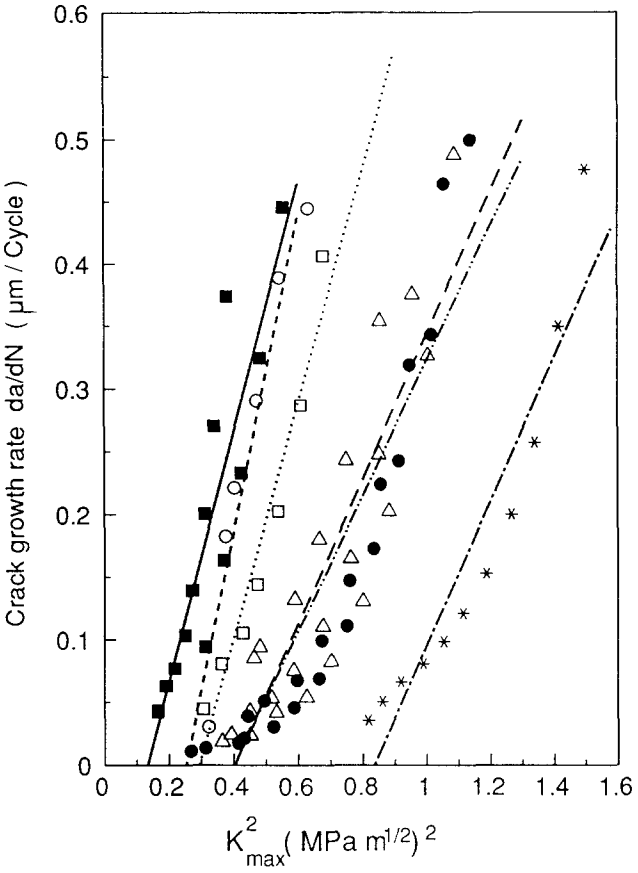

Figure 6 Fatigue crack growth of rubber-toughened epoxy resin plotted in accordance with equation (3) at 40°C and 5 Hz. The symbols are the same as in *Figure 5*

'bad' data point cannot be ignored arbitrarily. Hence, from equations (4) and (5) and using $E=2.04$ GPa (ref. 9) and $K_c=1.52$ MPa m$^{1/2}$ from *Figure 4* and $F(R)=S(R)/S(0)$, the determination of the fracture parameters α, σ_0 and δ_c can be obtained. *Table 2* shows these calculated parameters. The predicted threshold values ΔK_{th} agree reasonably well with the experimental results. The damage stress σ_c is of the order of 40 MPa and $\delta_c=1.78$ μm. Corresponding analysis has been performed for the fatigue crack growth data at 60°C and 5 Hz. We obtain $K_0=0.11$ MPa m$^{1/2}$, $\alpha\sigma_0\approx 18$ MPa and $\delta_c\approx 4.7$ μm. Again, the predicted threshold values ΔK_{th} compare reasonably well with experimental data. *Table 3* gives the relevant parametric values using equations (4) to (6), $K_c=2.48$ MPa m$^{1/2}$ and $E=1.8$ GPa. The dependence of S on R indicates that the functional form of $S(R)$ is $(1-R)^n$ where $n\approx 0.8$ at $T=40$°C and $n\approx 1.2$ at $T=60$°C, which according to Williams' model indicates that shear yielding at the advancing crack tip of the line zone might be the major fatigue mechanism[22] in this material at these temperatures.

Wu–Mai–Cotterell fatigue damage model. The proposed model[24] assumes that the material elements in a Dugdale yield strip of unit width (in front of the crack tip) on entering the reversing plastic zone suffer accumulative damage. A plastic hysteresis energy criterion for fatigue damage according to the Coffin–Manson equation is

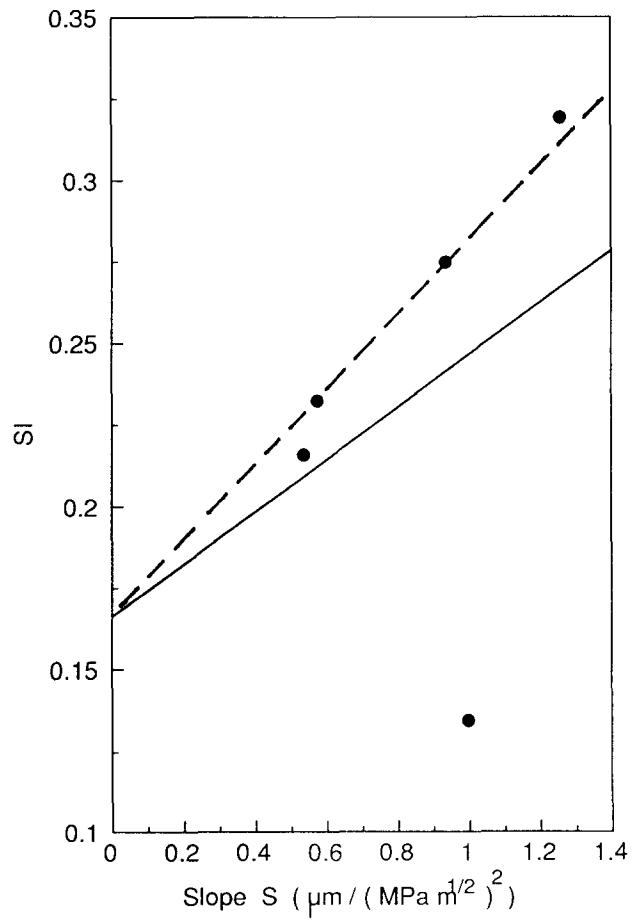

Figure 7 A plot of *SI versus S* for rubber-toughened epoxy resin at 40°C and 5 Hz

Table 2 Fatigue crack growth parameters at 40°C and 5 Hz ($K_c = 1.52$ MPa m$^{1/2}$, $K_0 = 0.30$ MPa m$^{1/2}$, $E = 2.04$ GPa, $\delta_c = 1.78$ μm)

R	α	σ_0 (GPa)	$\alpha\sigma_0$ (MPa)	ΔK_{th}(theory) (MPa m$^{1/2}$)	ΔK_{th}(exp.) (MPa m$^{1/2}$)
0.05	0.018	0.597	11	0.35	0.40
0.10	0.080	0.638	51	0.45	–
0.30	0.074	0.633	47	0.38	–
0.50	0.069	0.630	44	0.32	0.30
0.60	0.064	0.627	40	0.26	–
0.70	0.163	0.701	114	0.28	–

Table 3 Fatigue crack growth parameters at 60°C and 5 Hz ($K_c = 2.48$ MPa m$^{1/2}$, $K_0 = 0.11$ MPa m$^{1/2}$, $E = 1.8$ GPa, $\delta_c = 4.7$ μm)

R	α	σ_0 (GPa)	$\alpha\sigma_0$ (MPa)	ΔK_{th}(theory) (MPa m$^{1/2}$)	ΔK_{th}(exp.) (MPa m$^{1/2}$)
0.10	0.020	0.720	15	0.37	0.29
0.20	0.033	0.729	24	0.38	–
0.50	0.027	0.725	20	0.32	0.25
0.70	0.029	0.726	20	0.26	–

given by:

$$\Delta\varepsilon_p(2N_f)^{-c} = 2\varepsilon_f' \tag{7}$$

where $\Delta\varepsilon_p$ is the plastic strain range, N_f is the number of cycles to failure, c and ε_f' are the fatigue ductility exponent and coefficient, respectively. For many metals and alloys $c \approx -0.5$. In Dugdale-type material with a constant yield strength σ_y, the plastic strain energy $\Delta W = \sigma_y \Delta\varepsilon_p$ and equation (7) may be rewritten as:

$$(\Delta W)^\beta N_f = D \tag{8}$$

where $\beta = -1/c$ and $D = (2\sigma_y\varepsilon_f')^\beta/2$ are constants. Using Miner's linear cumulative damage law for varying-amplitude strain-controlled fatigue we have:

$$\int_0^{N_f} (\Delta W)^\beta \, dN = D \tag{9}$$

and D can be independently determined by the following equation:

$$D = \tfrac{1}{4}(\sigma_y\delta_c/h)^\beta = \tfrac{1}{4}(K_c^2/Eh)^\beta \tag{10}$$

by assuming equation (8) to apply to monotonic fracture at which $N_f = 1/4$ cycle and h is the width of plastic yield strip. In Dugdale's model the plastic yield strip has zero thickness, but to convert displacement to strain we need to assume a finite thickness of this plastic line zone. To include crack closure in the fatigue model we have used the residual plastic stretch analysis of Budiansky and Hutchinson for a Dugdale crack[30] and computed this for varying R ratios. A fatigue threshold ΔK_0 and its corresponding plastic stretch $\Delta\delta_0$ below which no fatigue damage occurs is also assumed in the model. Thus, the fatigue damage law becomes:

$$\int_0^{N_f} \sigma_y^\beta(\Delta\delta - \Delta\delta_0)^\beta \, dN = \tfrac{1}{4}(K_c^2/E)^\beta \tag{11}$$

To consider crack *nucleation* after N_i cycles under a plastic stretch range $\Delta\delta_s$ we obtain:

$$\sigma_y^\beta(\Delta\delta_s - \Delta\delta_0)^\beta N_i = \frac{1}{4}\left[\left(\frac{K_c^2}{E}\right)^\beta - \left(\frac{K_m^2}{E}\right)^\beta\right] \tag{12}$$

where $K_m = \Delta K/(1-R)$, $\Delta\delta_0 = \Delta K_0^2/E\sigma_y$ and $\Delta\delta_s = (\Delta K)^2/2E\sigma_y$. Hence solving equation (12) the crack nucleation cycle N_i for a given ΔK is given by:

$$N_i = \frac{2^{\beta-2}\{[(1-R)K_c]^{2\beta} - (\Delta K)^2\beta\}}{(1-R)^{2\beta}[(\Delta K)^2 - 2(\Delta K_0)^2]^\beta} \tag{13}$$

The threshold ΔK_{th}^s to initiate a *stationary* crack is:

$$\Delta K_{th}^s = \sqrt{2}\Delta K_0 \tag{14}$$

For the *propagation* of a steady crack we need to consider the residual plastic stretch δ_m that is left behind in the crack wake region, which is a function of R and position x within the plastic zone length ω. Without going into mathematical details of the derivations, we give the final result below for the *FCG* rate equation[24]:

$$\frac{d(a/\omega_c)}{dN} = \frac{4(\Delta K/K_c)^{2\beta+2}}{(1-R)^{2\beta} - (\Delta K/K_c)^{2\beta}} \frac{f_1(R)}{(1-R)^2} I(\beta, R) \tag{15}$$

where $I(\beta, R)$ is an integral to be evaluated and the critical plastic zone length is:

$$\omega_c = \frac{\pi}{8}\left(\frac{K_c}{\sigma_y}\right)^2 \tag{16}$$

Also, the condition that the effective plastic stretch range must be bigger than $\Delta\delta_0$ gives the fatigue crack growth threshold ΔK_{th} for the *propagating* crack, i.e.

$$\Delta K_{th} = \frac{1-R}{[1-f_2(R)]^{1/2}}\Delta K_0 \tag{17}$$

The expressions for $f_1(R)$ and $f_2(R)$ were derived earlier by Wu *et al.*[24] following the method of Budiansky and

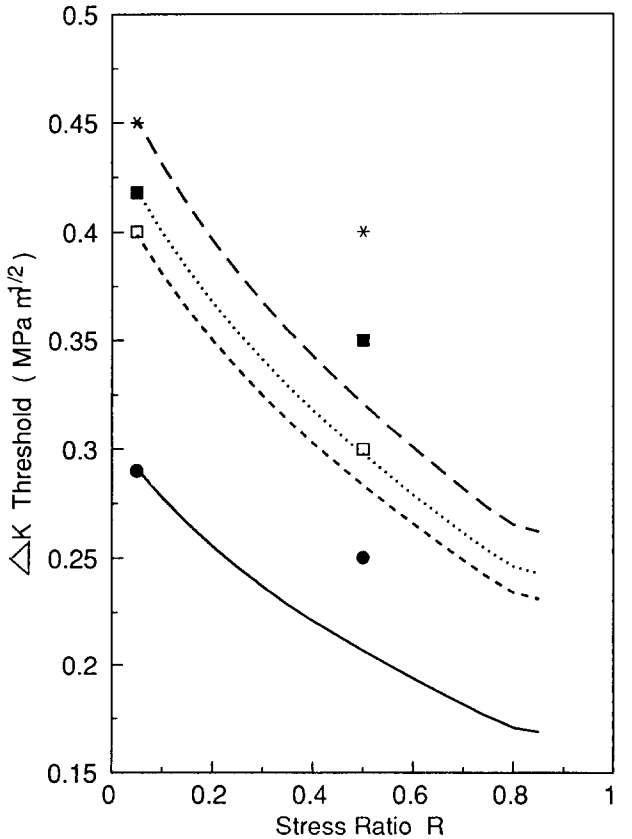

Figure 8 Fatigue threshold plotted against stress ratio at 60°C (●), 40°C (□), 20°C (■) and −20°C (*). Theoretical curves are from equation (17): (——) 60°C, (– – –) 40°C, (· · · ·) 20°C, (— — —) −20°C

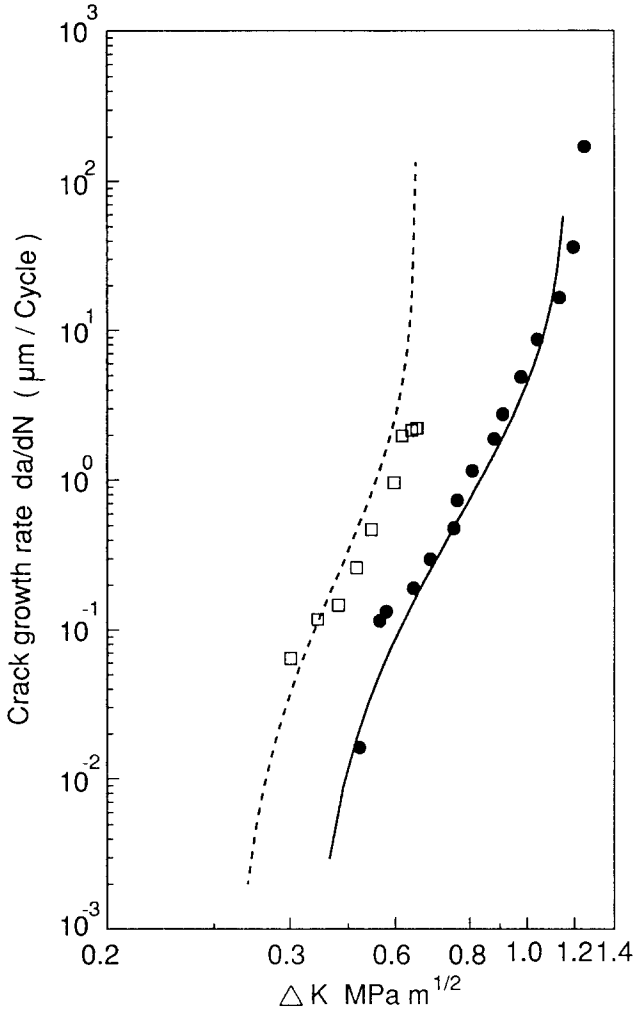

Figure 9 Fatigue crack growth in rubber-toughened epoxy resin at −20°C for $R=0.1$ (●), 0.5 (□) (experimental) and $R=0.1$ (——), 0.5 (– – –) (damage model based on $\beta=1.39$)

Hutchinson[30]. Thus, we have:

$$f_1(R)=0.093+0.026R-0.352R^2+0.234R^3$$

$$f_2(R)=0.856-0.015R+0.416R^2-0.252R^3$$

To determine ΔK_0 we fit equation (17) to an experimental value ΔK_{th} at the lowest R ratio. This ΔK_0 is then used to evaluate ΔK_{th} for all other R ratios. These predicted ΔK_{th} curves are given in *Figure 8* and agreement with the limited experimental data is not really good, though the trend is well predicted. However, it is very likely that in our experiments the true fatigue thresholds have not yet been obtained. Now, knowing ΔK_0 and K_c (from *Figure 8*) for each test temperature, we can determine the most appropriate β value that best fit the fatigue crack growth data at the lowest R ratio using equation (15). These same parameters are then used to correlate the fatigue crack growth rates at other stress ratios based on equation (15). *Figures 9* to *12* represent such correlated curves for −20, 20, 40 and 60°C. In general, it may be said that, unlike equation (2), there is reasonably good agreement with the experimental results for the *full range* of *FCG* rates. The trends of fatigue thresholds are also quite well modelled, i.e. ΔK_{th} decreasing with increasing R. The values of β vary between 1.11 and 1.43, which do not compare well with the range of values between 2 and 4 reported in the literature for the Coffin–Manson law for plastics. This discrepancy in the β values will have to be investigated in more detail.

It is realized that in the Coffin–Manson law experiments, as shown by Murakami[31], the lifetime expended in crack propagation is about 90% of the total number of cycles to failure. Hence, there is much strain localization at the crack tip so that $\Delta\varepsilon_p$ is much *larger* than the nominal $\Delta\varepsilon_p$ applied to the sample. If Coffin–Manson equations (7) and (8) are used to describe failure then β (or c) should be *smaller*. Murakami has argued that the Coffin–Manson law exponent is related to the singular strain distribution of a small crack in a gross plastic field. He shows that the singular strain for a small crack is given by:

$$\Delta\varepsilon_y \propto r^{-(0.5-0.7)} \tag{18}$$

using finite-element analysis. Consequently, he concludes that the exponent of the Coffin–Manson law must be about 0.5 to 0.7, giving β values of 1.4 to 2.0. Our estimated β values for the rubber-toughened epoxy resin, however, fall slightly below the low end of Murakami's results.

Another reason is due to our assumption in the model that the finite width h of the plastic strip is independent of the applied K. But in reality h must be proportional to $(K_m/\sigma_y)^{2\nu}$ where ν is less than unity. Thus β in the *FCG* equation (15) is replaced by $\beta(1-\nu)$, leading to larger values for the *real* β of the Coffin–Manson law.

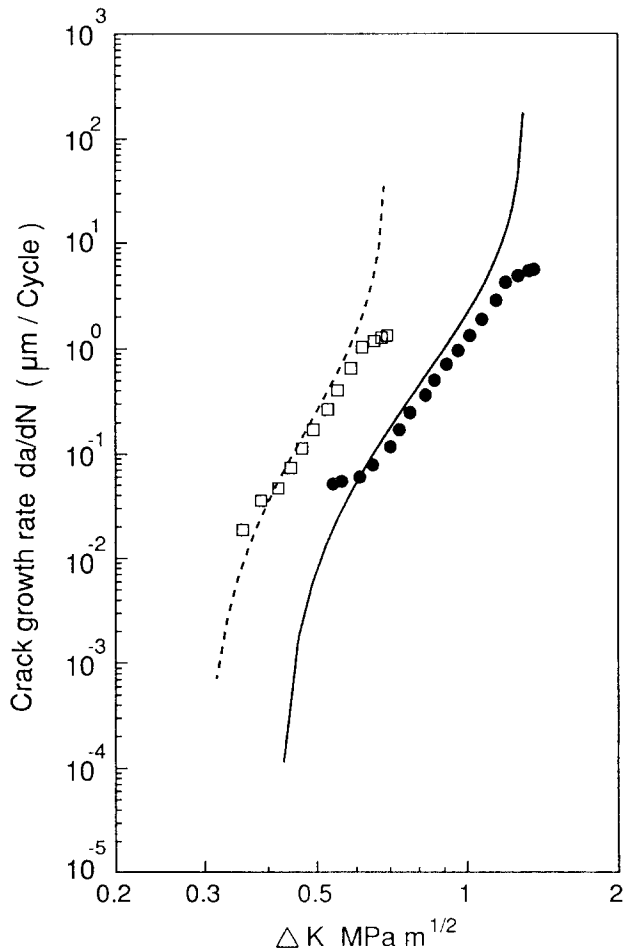

Figure 10 Fatigue crack growth in rubber-toughened epoxy resin at 20°C for $R=0.05$ (●), 0.5 (□) (experimental) and $R=0.05$ (——), 0.5 (– – –) (damage model based on $\beta=1.11$)

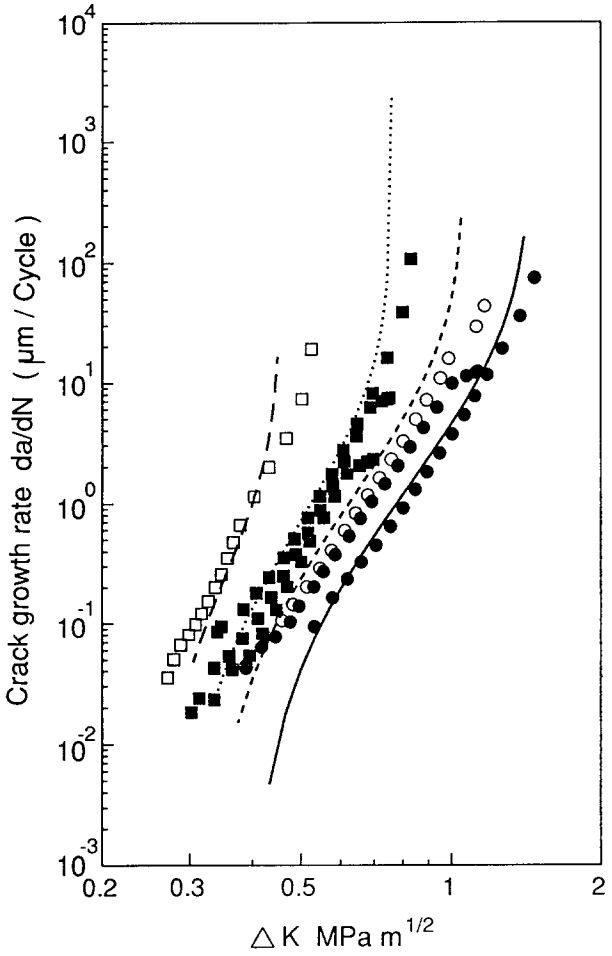

Figure 11 Fatigue crack growth in rubber-toughened epoxy resin at 40°C for $R=0.05$ (●), 0.3 (○), 0.5 (■), 0.7 (□) (experimental) and $R=0.05$ (——), 0.3 (– – –), 0.5 (· · · ·), 0.7 (— — —) (damage model based on $\beta=1.43$)

As we are unable to identify β with the power-law exponent of the Coffin–Manson equation, we propose to treat β as an adjustable parameter to correlate *FCG* rates at all R ratios. Its usefulness depends on its ability to make accurate *FCG* correlations with experimental results. Also, although the model is derived based on the Dugdale plane-stress assumptions, its application to the rubber-toughened epoxy resin subjected to cyclic fatigue in plane strain is apparently valid. This comment of course applies equally to the Williams' model, which is also based on the Dugdale crack solutions.

A few comments may be made about the Williams' two-stage line zone model and the Wu–Mai–Cotterell fatigue damage model, even though both approaches are very similar. Whilst Williams' model relies on a critical crack-tip opening displacement δ_c fracture criterion that has been quite severely criticized[29] (because it does not agree with experimental measurements on δ_c during fatigue crack growth), the Wu–Mai–Cotterell model makes no such assumption and is formulated on a physically sound accumulative damage criterion. There are also more parameters (i.e. α, K_0, δ_c and $F(R)$) to determine in Williams' model (which are not always easy as shown in *Figure 7* for K_0) than in our model (i.e. ΔK_0 and β). It seems that since these parameters are determined from very small *FCG* rates (*Figure 6*), they are unable to describe the *full range* of *FCG* data (shown in *Figure 5*). Conversely, the same *FCG* data correlate very well (*Figure 11*) with the Wu–Mai–Cotterell model using only one set of β and ΔK_0 values. We believe that the present model is simpler to use and requires only the evaluation of two fracture parameters, ΔK_0 and β. The physical connection of β to the exponent of the Coffin–Manson equation is, however, not clear at this stage.

CONCLUSIONS

The effects of temperature and stress ratios on the fatigue crack growth rates in rubber-toughened epoxies have been investigated. The results show that at a given stress ratio there is no definite trend for the effect of temperature. However, increasing the stress ratio at each test temperature increases the fatigue crack growth rate. Representing the data in terms of the Paris power law gives wide variations in the parameters A and m, and it is difficult to assign physical significance to their values. The use of Williams' two-stage plastic line zone model gives the fracture parameters at different temperatures, which do provide a physical basis for the fatigue mechanisms involved. A new mechanistic model due to Wu *et al.* that expresses the fatigue crack growth data in terms of the evolution and accumulation of damage due to the cyclic plastic strain in the reversed plastic zone is tested. There is good agreement between the calculated results and experimental data but the Coffin–Manson

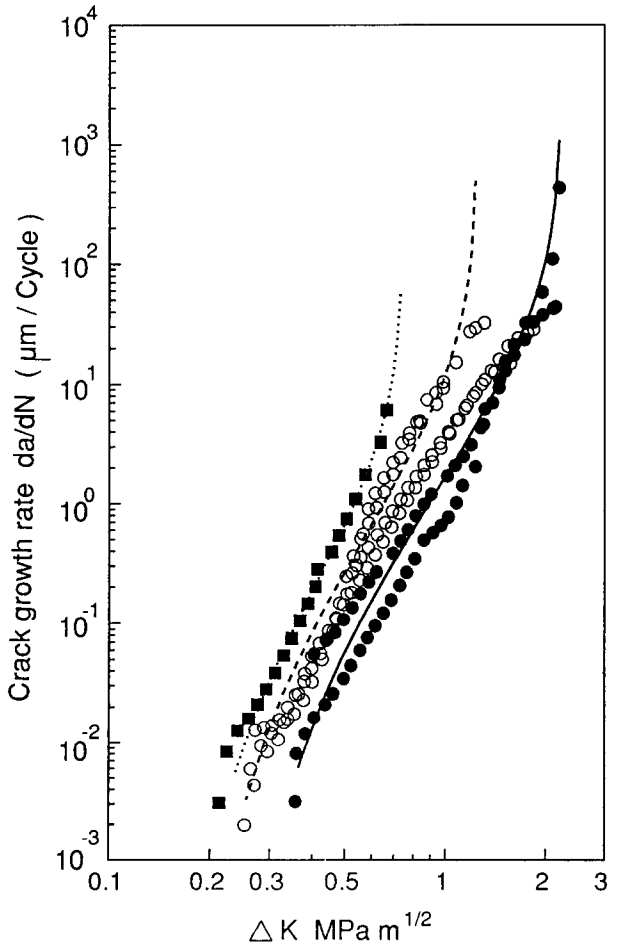

Figure 12 Fatigue crack growth in rubber-toughened epoxy resin at 60°C for $R=0.1$ (●), 0.5 (○), 0.7 (■) (experimental) and $R=0.1$ (——), 0.5 (– – –), 0.7 (· · · ·) (damage model based on $\beta=1.25$)

law exponent does not compare well with those values reported for plastics materials. Possible reasons for the discrepancy are given and discussed. It is finally concluded that the Wu–Mai–Cotterell model is simpler to use and gives a better description of the full range of fatigue crack growth data.

ACKNOWLEDGEMENTS

The authors wish to acknowledge the financial support of this work by the Aeronautical Research Laboratory, Defence Science and Technology Organisation, Australia, with Dr L. R. F. Rose as Program Coordinator. The experimental work was performed by M. E. Dunne and C. Engdahl. M. M. Abou-Hamda is supported by an Overseas Postgraduate Research Scholarship tenable at the University of Sydney.

REFERENCES

1 Bucknall, C. B. 'Toughened Plastics', Applied Science, London, 1977
2 Siebert, A. R. in 'Rubber-Modified Thermoset Resins' (Eds C. K. Riew and J. K. Gilham), Adv. Chem. Ser. 208, American Chemical Society, Washington, DC, 1984, pp. 179–191
3 Pearson, R. A. and Yee, A. F. in 'Tough Composite Materials', NASA Langley Research Center, Virginia, Noyes Publications, New Jersey, 1985, pp. 157–177
4 Hertzberg, R. A. and Manson, J. A. 'Fatigue of Engineering Plastics', Academic Press, New York, 1980
5 Maxwell, D. and Young, R. J. *J. Mater. Sci. Lett.* 1984, **3**, 9
6 Sultan, J. N. and McGarry, F. J. *Polym. Eng. Sci.* 1973, **13**, 29
7 Kinloch, A. J. and Hunston, D. L. *J. Mater. Sci. Lett.* 1986, **5**, 1207
8 Yee, A. F. and Pearson, R. A. *J. Mater. Sci.* 1986, **15**, 2462
9 Low, I.-M., Mai, Y.-W., Bandyopadhyay, S. and Silva, V. M. *Mater. Forum* 1987, **10**, 241
10 Bandyopadhyay, S., Silva, V. M., Low, I.-M. and Mai, Y.-W. *Plast. Rubb. Process. Applic.* 1988, **10**, 193
11 Sutton, S. A. *Eng. Fract. Mech.* 1974, **6**, 587
12 Kim, S. L., Skibo, M. D., Manson, J. A., Hertzberg, R. W. and Janiszewski, J. *Polym. Eng. Sci.* 1978, **18**, 1093
13 Mizutani, K. and Iwatasu, T. *Polym. Eng. Sci.* 1983, **23**, 183
14 Shah, D. N., Attala, G., Manson, J. A., Connelly, G. M. and Hertzberg, R. W. in 'Rubber-Modified Thermoset Resins' (Eds C. K. Riew and J. K. Gilham), Adv. Chem. Ser. 208, American Chemical Society, Washington, DC, 1984, pp. 117–135
15 Manson, J. A., Hertzberg, R. W., Connelly, G. M. and Hwang, J. in 'Multicomponent Polymer Materials' (Eds D. R. Paul and L. H. Sperling), Adv. Chem. Ser. 211, American Chemical Society, Washington, DC, 1986, pp. 291–312
16 Hwang, J. F., Manson, J. A., Hertzberg, R. W., Miller, G. A. and Sperling, L. H. *Polym. Eng. Sci.* 1989, **29**, 1477
17 Wang, X., Sehanobish, K. and Moet, A. *Polym. Compos.* 1988, **9**, 165
18 Kinloch, A. J. and Young, R. J. 'Fracture Behaviour of Polymers', Applied Science, London, 1983
19 Paris, P. C. and Erdogan, F. *J. Basic Eng. Trans., ASME (D)* 1963, **85**, 528
20 Williams, J. G. *J. Mater. Sci.* 1977, **12**, 2525
21 Mai, Y.-W. and Williams, J. G. *J. Mater. Sci.* 1979, **14**, 1933
22 Osorio, A. M. B. A. and Williams, J. G. in 'Advances in Fracture Research' (Eds D. Francois *et al.*), Vol. 1, Pergamon Press, Oxford, 1981, pp. 435–448
23 Yap, O. F., Mai, Y.-W. and Cotterell, B. in 'Advances in Fracture Research' (Eds D. Francois *et al.*), Vol. 1, Pergamon Press, Oxford, 1981, pp. 449–456
24 Wu, S.-X., Mai, Y.-W. and Cotterell, B. *Int. J. Fract.* 1992, **57**, 253
25 Mai, Y.-W. and Kerr, P. R. *J. Mater. Sci. Lett.* 1984, **3**, 971
26 Mai, Y.-W. and Kerr, P. R. *J. Mater. Sci.* 1985, **20**, 2199
27 Kinloch, A. J., Gilbert, D. G. and Shaw, S. J. *J. Mater. Sci.* 1986, **21**, 1051
28 Chan, L. C., Gilham, J. K., Kinloch, A. J. and Shaw, S. J. in 'Rubber-Modified Thermoset Resins' (Eds C. K. Riew and J. K. Gilham), Adv. Chem. Ser. 208, American Chemical Society, Washington, DC, 1984, pp. 235–261
29 Döll, W. in 'Crazing in Polymers' (Ed. H. H. Kausch), Adv. Polym. Sci. 51/52, Springer-Verlag, Berlin, 1983, pp. 105–168
30 Budiansky, B. and Hutchinson, J. W. *J. Appl. Mech.* 1978, **45**, 267
31 Murakami, Y. in 'Low Cycle Fatigue' (Eds H. D. Solomon *et al.*), ASTM STP 942, ASTM, Philadelphia, 1988, pp. 1048–1065